Lattice Contraction Driven Insulator-Metal Transition in the $d = \infty$ Local Approximation

Pinaki Majumdar and H. R. Krishnamurthy*
Department of Physics, Indian Institute of Science, Bangalore 560 012, India
(Received 29 April 1994)

We study the effects of lattice contraction on insulator-metal transitions in strongly correlated systems, in the context of the $d = \infty$, iterated perturbation theory approximation for the half-filled Hubbard model. We compute the phase diagram in the pressure-temperature plane for the paramagnetic metal to paramagnetic insulator transition. We present results for conductivity jumps across the transition and for the variation in conductivity with pressure and temperature in either phase. Our results agree qualitatively with experimental data on transition metal oxides.

PACS numbers: 71.27.+a, 71.10.+x, 71.28.+d, 74.20.Mn

The phenomena associated with correlation induced metal-insulator (M-I) transitions, such as in transition metal oxides, have now been known for many decades [1,2]. However, a detailed and quantitative understanding of these has remained elusive, in spite of enormous theoretical effort [1,2], because of the difficulties in solving the strongly correlated electron problem that is at the root of these phenomena. Recently there has been exciting progress on this latter front because of the development of the infinite-dimensional, local approximation [3–8]. In the light of these developments, in this paper we reexamine lattice contraction effects in correlation induced M-I transitions. Such effects have been looked at earlier [9] only in the context of the Hubbard (III) approximation [10].

Specifically, we show that systems described by purely electronic models with strong correlations, such as the Hubbard model at half filling, are intrinsically unstable with respect to lattice contraction effects. Such instabilities lead to a first order transition from the para insulator to a para metal at temperatures below a critical temperature T_c, but above the purely electronic M-I transition temperature T^*. Using the iterated perturbation theory (IPT) approach pioneered by Georges and Kotliar [4], we present the first detailed study of such transitions, including the calculation of conductivity jumps across the transition.

The compressional instability of the model (conduction) electronic systems alluded to above arises due to the dependence of Ω_e, the thermodynamic (grand) potential of the model, on the bandwidth parameter $D(v)$, which is typically a strong function of the unit cell volume v. The compressibility is given by

$$\kappa_e \equiv \frac{\partial^2 \Omega_e}{\partial v^2} = \left(\frac{\partial \Omega_e}{\partial D}\right)\left(\frac{\partial^2 D}{\partial v^2}\right) + \left(\frac{\partial^2 \Omega_e}{\partial D^2}\right)\left(\frac{\partial D}{\partial v}\right)^2. \quad (1)$$

Typically, $\partial^2 D/\partial v^2$ is positive [11], and $\partial \Omega_e/\partial D$ and $\partial^2 \Omega_e/\partial D^2$ are negative (cf. Fig. 2 and calculations below), hence $\kappa_e < 0$. In the real physical system, there is a positive contribution to the compressibility, κ_l, coming from the volume dependence of the site energies of the conduction electrons, the other (core) electrons, and from the ions, such that at high temperatures $\kappa_{\rm tot} = \kappa_e + \kappa_l > 0$ and the system is stable. *However, at low temperatures $|\kappa_e|$ becomes very large and may even diverge as $T \longrightarrow T^*$ and $D \longrightarrow D^*$.* For example, in the IPT approach κ_e diverges at $T^* \simeq 0.05D^*$, $D^* \simeq 0.33U$ for the following reasons. Below T^* there is a first order M-I transition, with both metallic and insulating solutions to the IPT equations (see below) existing [8] inside the solid line in the inset of Fig. 1. Across this transition the momentum distribution function $\langle n_{\vec{k}} \rangle$ changes abruptly, from a Fermi-liquid form on the metallic side to a smooth function of $\epsilon_{\vec{k}}$ on the insulating side; hence $D\partial\Omega_e/\partial D \equiv \langle E_{\rm kin} \rangle$ (where $E_{\rm kin}$ the kinetic energy of the conduction electrons) changes discontinuously across the M-I transition as shown in Fig. 2. As $T \longrightarrow T^*$ from below the discontinuity in $\partial\Omega_e/\partial D$ decreases, leading to a divergence of $\partial^2\Omega_e/\partial D^2$ at T^*. The same divergence in $\partial^2\Omega_e/\partial D^2$ and consequently in κ_e will show up as $T \longrightarrow T^*$ from above, as indicated in the inset of Fig 2. Hence $\kappa_{\rm tot}$ can become negative in the region $D(v) \simeq D^*$ below a critical temperature T_c ($> T^*$). This is an unstable condition which the physical system avoids by generating a first order M-I transition accompanied by a

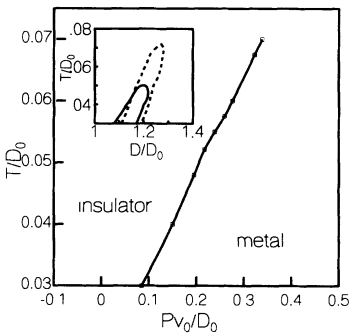

FIG. 1. *P-T* phase diagram computed for $\kappa_l v_0^2/D_0 = 6.0$. Inset: Discontinuity in bandwidth across the transition. The solid line indicates the limits of metastability in the purely electronic scenario, while the dashed line denotes the boundary of coexistence in the presence of lattice coupling.

0031-9007/94/73(11)/1525(4)$06.00

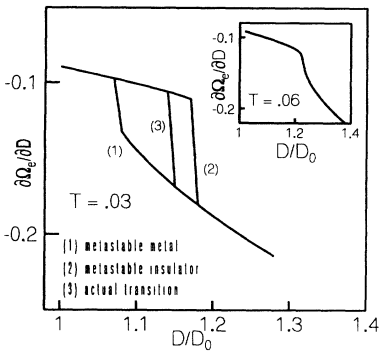

FIG. 2. $\partial\Omega_e/\partial D$ for $T < T^*$, $U = 3.0$. Inset: $\partial\Omega_e/\partial D$ for $T = 0.06 > T^*$, indicating a sharp crossover.

discontinuous volume change straddling the unphysical region where $\kappa_{\text{tot}} < 0$, as shown in the inset of Fig. 1. The transition is accompanied by sharp changes in the electronic spectrum and the transport properties of the system, as indicated by the conductivity jumps across the transition shown in Fig. 3.

For the detailed quantitative study of the M-I transition scenario outlined above, leading to the results in Figs. 1–3 for the half-filled Hubbard model, we have relied on the $d = \infty$ local approximation in the IPT scheme [12]. The approximation has been well detailed and motivated elsewhere [8]. We use the Hamiltonian

$$\hat{H} = -\sum_{\substack{\langle ij\rangle \\ \sigma}}(t_{ij} + \mu\delta_{ij})c^{\dagger}_{i\sigma}c_{j\sigma} + U\sum_i n_{i\uparrow}n_{i\downarrow} \qquad (2)$$

with $\mu = U/2$ ensuring half filling. In the local approximation the spectral properties are determined from the solution of a self-consistently embedded impurity problem which involves a single site electronic degree of freedom with a retarded "bare" local propagator $\mathcal{G}(i\omega_n)$ [$\omega_n = (2n + 1)\pi T$ are the fermionic Matsubara frequencies] and interaction U as in (2). From the Dyson equation, the full local propagator is

$$G^{-1}(i\omega_n) = \mathcal{G}^{-1}(i\omega_n) - \Sigma(i\omega_n), \qquad (3)$$

where the self-energy $\Sigma(i\omega_n)$ is some functional of $\mathcal{G}(i\omega_n)$ and of U, e.g., as given by the perturbation series in powers of U [13]. The connection to the lattice problem is made via the self-consistent embedding condition: The impurity self-energy is the same as the lattice self-energy (the local $d = \infty$ approximation which neglects the momentum dependence of Σ), and the full G is the local band propagator

$$G(i\omega_n) = G_{ii}(i\omega_n) = \int_{-D}^{+D} \frac{d\epsilon_k \rho_0(\epsilon_k)}{i\omega_n + \mu - \epsilon_k - \Sigma(i\omega_n)}. \qquad (4)$$

Here $\rho_0(\epsilon)$ is the noninteracting band density of states (DOS) and D its half bandwidth.

The bottleneck in the whole $d = \infty$ local approximation program is the problem of calculating the impurity self-energy $\Sigma(i\omega_n)$ given an arbitrary bare propagator $\mathcal{G}(i\omega_n)$. In the IPT scheme, one approximates Σ by the leading nontrivial perturbative term [13]

$$\Sigma(i\omega_n) = U^2\int_0^{\beta} d\tau e^{i\omega_n\tau}\mathcal{G}^3(\tau) + \frac{U}{2} \qquad (5)$$

where $\mathcal{G}(\tau) = \beta^{-1}\sum_n \mathcal{G}(i\omega_n)e^{-i\omega_n\tau}$, as usual. For concreteness we use this in the context of the semicircular DOS $\rho_0(\epsilon) = (2/\pi D)\sqrt{1 - (\epsilon^2/D^2)}$ whence the self-consistency condition (4) becomes

$$G(i\omega_n) = 2\left[z_n + \sqrt{z_n^2 - D^2}\right]^{-1},$$
$$z_n \equiv i\omega_n + \mu - \Sigma(i\omega_n). \qquad (6)$$

We solve the set of equations (3), (5), and (6) numerically in the Matsubara formulation by a simple iterative scheme, as well as directly in the real frequency domain (by a procedure discussed below). Thermodynamic properties are computed from $G(i\omega_n)$ and $\Sigma(i\omega_n)$ at convergence for a particular parameter set (U, D, T), while the dc conductivity is calculated using the real-frequency objects.

Although there exist formulas relating the thermodynamic potential Ω_e to $G(i\omega_n)$ and $\Sigma(i\omega_n)$, we have found it far more convenient to compute $\partial\Omega_e/\partial D$ directly as follows. Writing the kinetic energy part of (2) as D times a dimensionless form, it is easy to see that $D(\partial\Omega_e/\partial D) = \sum_{k,\sigma}\epsilon_k\langle n_{k,\sigma}\rangle$. Using $\langle n_{k,\sigma}\rangle = \beta^{-1}\sum_n G_\sigma(\vec{k}, i\omega_n)$ and the local approximation to the self-energy, one gets for the semicircular DOS

$$D\frac{\partial\Omega_e}{\partial D} = \frac{2}{D\beta}\sum_n \frac{z_n - \sqrt{z_n^2 - D^2}}{z_n + \sqrt{z_n^2 - D^2}}. \qquad (7)$$

We compute $\partial\Omega_e/\partial D$ for a discrete set of D values between 0.1 and 10, closely sampled in the crossover region

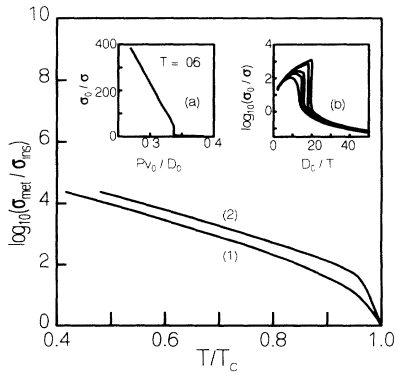

FIG. 3. Conductivity ratio across the transition for $\kappa_l v_0^2/D_0 = 6$ (1), and 8 (2). Inset (a): Variation in ρ with P at fixed T, close to T_c. Inset (b): Variation in ρ with $1/T$ for various P (from the lowest curve up $Pv_0/D_0 = 0.38, 0.32, 0.29, 0.27, 0.24, 0.19$).

$D \simeq 1.0$ where the IPT gives rise to a M-I transition [cf. Fig. 1]. U is fixed at 3.0 and sets the energy scale in the problem. As noted before [8] the IPT scheme admits metastable solutions in the crossover region ($D \simeq 1.0$, $T < T^* \simeq 0.05$). The metastable solutions are generated by starting deep in the metallic-insulating state and feeding in the converged $\Sigma(i\omega_n)$ from one parameter set as starting self-energy for the iterations for the next set. The true $\partial\Omega_e/\partial D$ curve is obtained by tracking both solutions in the crossover region and determining the transition point by comparing the corresponding free energies. Figure 2 shows the variation in $\partial\Omega_e/\partial D$ for an insulating and metallic solution in the crossover region and for the actual transition between these solutions. Above $T^* = 0.05$ there exists only one solution of the IPT equations as we scan in D at fixed U and T. For $T > T^*$ the variation in $\partial\Omega_e/\partial D$ with D is continuous but very sharp in the crossover region (see inset in Fig. 2), leading to a large negative $\partial^2\Omega_e/\partial D^2$ as discussed earlier. The crossover in $\partial\Omega_e/\partial D$ (which naturally couples to the lattice in our scenario) shifts to larger D with increasing temperature, much beyond T^*.

Next we couple in the lattice by introducing a volume dependence of D of the form $D(v) = D_0 \exp[-\gamma(v - v_0)/v_0]$ (we set $D_0 = 1.0$, the reference value) and an energy cost for lattice deformation of the form $E(v) = \frac{1}{2}\kappa_l(v - v_0)^2$. Then one gets, by the mechanism outlined earlier, a first order M-I transition below a critical temperature T_c determined by κ_l and γ. v_i and v_m, the specific volumes on the insulating and metallic side of the transition, respectively (and D_i and D_m the corresponding bandwidths), are fixed by the standard Maxwell construction. In terms of the Gibbs free energy

$$G(P, v) = P(v - v_0) + \Omega_e[D(v)] + \mu + E(v) \quad (8)$$

one has the following conditions: (*i*) $G(P, v_i) = G(P, v_m)$ and (*ii*) $(\partial G/\partial v)_{v_i} = (\partial G/\partial v)_{v_m} = 0$ from which v_i and v_m can be computed. The volume jump $v_i - v_m$ becomes smaller as T increases above T^* and vanishes at the critical point T_c determined by the additional condition $\partial^2 G/\partial v^2 = 0$. For the choice of parameters $\gamma = 2$ and $\kappa_l v_0^2 = 6$ which we have studied in detail, $T_c = 0.075$. The phase diagram and the jumps in D computed in this scheme are shown in Fig. 1.

We next discuss the transport properties, specifically the conductivity jumps, across the first order M-I transition. For computing these, we found that the Matsubara frequency formalism discussed above is not so convenient (although the IPT equations converge easily because the functions involved are not singular), because of the well known problems [14] of analytic continuation to real frequencies. Hence to compute frequency dependent correlation functions we have set up and solved the IPT equations directly for the spectral functions (at both zero and finite temperature). From (5) we can write down an equation for the spectral function of Σ, $\rho_\Sigma \equiv -\pi^{-1}\mathrm{Im}\Sigma(\omega^+)$, directly in terms of the spectral function of $\mathcal{G}$, $\rho_\mathcal{G} \equiv -\pi^{-1}\mathrm{Im}\mathcal{G}(\omega^+)$. We use this equation, the Kramers-Kronig expression for Σ_r, namely $\Sigma_r(\omega) = -\int d\omega' \rho_\Sigma(\omega')(\omega - \omega')^{-1}$, the real frequency versions of the Dyson Eq. (3), and the consistency condition (6), to achieve self-consistency. The dc conductivity is calculated as [15]

$$\sigma_{\mathrm{dc}} = \sigma_0 D_0^2 \int d\epsilon_k \rho_{\mathrm{tr}}^0(\epsilon_k) \int d\omega A^2(\vec{k}, \omega) \frac{\partial}{\partial\omega}\{n_F(\omega)\}. \quad (9)$$

Here $\rho_{\mathrm{tr}}^0(\epsilon_k)$ is a "transport DOS" which in the $d = \infty$ limit essentially reduces to $\rho_0(\epsilon_k)$ [15], and σ_0 is a constant with dimensions of conductivity whose value [typically [15] 10^{-2} to 10^{-3} $(\mu\Omega\,\mathrm{cm})^{-1}$] depends on the details of the modeling of the conduction electrons (i.e., on material parameters, band structures, etc.). $A(\vec{k}, \omega)$ is the spectral function

$$A(\vec{k}, \omega) \equiv -\pi^{-1}\,\mathrm{Im}[\omega + \mu - \epsilon_k - \Sigma(\omega)]^{-1}. \quad (10)$$

Vertex parts are local [16] in the $d = \infty$ approximation, and hence vertex corrections completely drop out of the dc conductivity because of the odd parity of the velocity vertex (with respect to momentum) [17]. The conductivity ratio computed at various pressure, temperature values along the M-I coexistence curve is shown in Fig. 3 for two representative values of $\kappa_l v_0^2$. In the insets of Fig. 3 we also show the variation of the resistivity (σ_0/σ) with P for a fixed T (a), and with $1/T$ for various values of P (b), across the M-I transition. We note that the conductivity in the insulating phase is dominated by activated transfer between the Hubbard bands and at low temperature ($T < 0.03$) can be computed quite accurately using the zero temperature spectral functions.

It is worth comparing our results with the experimental data on the $(V_{1-x}Cr_x)_2O_3$ system which has been extensively studied [18–22]. Specifically *we focus on its paramagnetic M-I transition occurring at intermediate (200–400 K) temperatures*, which has almost a constant positive slope, $dT/dP \simeq 50$ K/kbar. [Within the IPT one cannot as reliably study the antiferromagnetic (AF) phase or the para metal to AF insulator transition which is much more spectacular.] The high-pressure–low-temperature phase (above the AF transition) is metallic, while the low-pressure–high-temperature phase is insulating. The measured volume jumps across the transition [18] are typically 1%, except as $T \longrightarrow T_c$; $\Delta v/v \simeq 0.013$ at $T \simeq 200$ K. The corresponding $s_i - s_m$, obtained using the Clausius-Clapeyron equation, is $\simeq 0.14$.

Clearly, our phase diagram, Fig. 1, is qualitatively consistent with these data. However, the typical T_c's we get with $D_0 = 1.0$ eV, and indeed T^* itself, are larger than the observed T_c. The $\Delta v/v$ for $\kappa_l v_0^2 = 6.0$ is typically much too large ($\simeq 3\%$ at $T = T_c/2$), but can

be made smaller by choosing larger $\kappa_l v_0^2$ values which also reduce T_c. Our calculated value for a typical entropy jump (at $T = T_c/2$ for $\kappa_l v_0^2 = 6.0$) is $s_i - s_m \simeq 0.21$, somewhat larger than the experimental value. In the para insulating phase, the $d = \infty$ approximation neglects the interaction between spin fluctuations [$J_{ij} \simeq t_{ij}^2/U \simeq (1/d)D^2/U$]; hence their contribution to the entropy would be overestimated. The resistivity ratio across the transition in the V_2O_3 system is typically 2–3 orders of magnitude [19,20] and drops sharply as $T \longrightarrow T_c$ in a way similar to Fig. 3. The observed variation [20] of ρ with P at constant T, and with $1/T$ at constant P, is qualitatively similar to the insets (a) and (b) in Fig. 3. However, in the experimental data, ρ in the metallic phase is predominantly T independent, due to disorder effects; though a component varying as aT^2 (with $a \simeq 0.03 - 0.04\ \mu\Omega\ \mathrm{cm/K^2}$, and increasing as P decreases) has been identified [19]. Our calculations for the metallic resistivity [inset (b) in Fig. 3] have no disorder component and do vary as aT^2, with a increasing as P decreases. A typical value for a is $\simeq (1.6 \times 10^{-4}/\sigma_0)\mu\Omega\ \mathrm{cm/K^2}$. If one takes $\sigma_0 \simeq 0.5 \times 10^{-2}\ (\mu\Omega\ \mathrm{cm})^{-1}$ [in the middle of the range $10^{-2} - 10^{-3}\ (\mu\Omega\ \mathrm{cm})^{-1}$ mentioned earlier] one gets $a \simeq 0.032\ \mu\Omega\ \mathrm{cm/K^2}$, in the right range.

In conclusion, we believe that the mechanism outlined here is responsible for the first order paramagnetic M-I transitions observed in transition metal oxides. The quantitative results are limited partly by the IPT scheme, and by the $d = \infty$ approximation, not to mention the limitations of the Hubbard model itself and the neglect of disorder and electron-phonon scattering effects. We hope to look at some of these issues in future work.

We thank T. V. Ramakrishnan, B. S. Shastry, A. K. Raychaudhuri, and D. M. Gaitonde for discussions and the Supercomputer Education and Research Center, Indian Institute of Science, for providing computational facilities. H. R. K thanks G. Kotliar for discussions regarding the IPT.

Note added.—A recent preprint by G. A. Thomas *et al.* [23] on optical conductivity measurements in V_2O_3 suggests that the $d = \infty$ approach to the Hubbard model coupled with lattice effects could be a reasonable starting point for describing V_2O_3. They extract a bandwidth $D_0 \simeq 0.4$ eV, which brings our T_c value $\simeq 0.08 D_0$ in closer correspondence with experiments.

*Also at Jawaharlal Nehru Center for Advanced Scientific Research, IISc campus, Bangalore 560 012, India.

[1] N. F. Mott, *Metal Insulator Transitions* (Taylor and Francis, London, 1974).
[2] For a recent review see T. V. Ramakrishnan, in *Current Topics in Condensed Matter and Particle Physics* (World Scientific, Singapore, 1991); also H. Hasegawa, Tech. Report of ISSP, Ser. A, No. 2090, 1989, and references therein.
[3] W. Metzner and D. Vollhardt, Phys. Rev. Lett. **62**, 324 (1989).
[4] A. Georges and G. Kotliar, Phys. Rev. B **45**, 6479 (1992).
[5] M. Rozenberg, X. Y. Zhang, and G. Kotliar, Phys. Rev. Lett. **69**, 1236 (1992).
[6] M. Jarrell, Phys. Rev. Lett. **69**, 168 (1992).
[7] A. Georges and W. Krauth, Phys. Rev. Lett. **69**, 1240 (1992).
[8] A. Georges and W. Krauth, Phys. Rev. B **48**, 7167 (1993).
[9] M. Cyrot and P. Lacour-Gayet, Solid State Commun. **11**, 1767 (1972).
[10] J. Hubbard, Proc. R. Soc. London A **281**, 401 (1964).
[11] W. A. Harrison, *Electronic Structure and Properties of Solids* (W. H. Freeman, San Francisco, 1980).
[12] In a recent preprint by M. Rozenberg, G. Moeller, and G. Kotliar, Rutgers, 1993 (unpublished), the zero temperature transition has been shown to be second order. This, however, does not modify our conclusions, which depend only on the finite temperature transition being of first order and ending at an upper critical point. The IPT describes these features reasonably well.
[13] K. Yosida and K. Yamada, Prog. Theor. Phys. **46**, 244 (1970).
[14] R. N. Silver, D. S. Sivia, and J. E. Gubernatis, Phys. Rev. B **41**, 2380 (1990).
[15] Th. Pruschke, D. L. Cox, and M. Jarrell, Europhys. Lett. **21**, 5 (1993); Phys. Rev. B **47**, 3553 (1993).
[16] E. Mueller-Hartmann, Z. Phys. B **74**, 507 (1989).
[17] A. Khurana, Phys. Rev. Lett. **64**, 1990 (1990).
[18] A. Jayaraman, D. B. McWhan, J. P. Remeika, and P. D. Dernier, Phys. Rev. B **2**, 3751 (1970).
[19] D. B. McWhan, A. Menth, J. P. Remeika, W. F. Brinkman, and T. M. Rice, Phys. Rev. B **7**, 1920 (1973).
[20] H. Kuwamoto, J. M. Honig, and J. Appel, Phys. Rev. B **22**, 2626 (1980).
[21] J. Spalek, A. Datta, and J. M. Honig, Phys. Rev. Lett. **59**, 728 (1987).
[22] S. A. Carter, T. F. Rosenbaum, J. M. Honig, and J. Spalek, Phys. Rev. Lett. **67**, 3440 (1992).
[23] G. A. Thomas *et al.* (to be published).